Journal of CO2 Utilization 97 (2025) 103136

Contents lists available at ScienceDirect

Journal of CO2 Utilization

journal homepage: www.elsevier.com/locate/jcou

Evaluation of single chamber electrochemical reduction of CO_2 to formate for application under biocompatible conditions

Zainab Ul [a,1], Mira Sulonen [a,b,2], Philip Haus [c,3], Paniz Izadi [c,4], Juan Antonio Baeza [a,*,5], Falk Harnisch [c,6], Albert Guisasola [a,7]

[a] GENOCOV, Departament d'Enginyeria Química, Biològica i Ambiental, Escola d'Enginyeria, Universitat Autònoma de Barcelona, Bellaterra (Cerdanyola del Vallès), Barcelona 08193, Spain
[b] VTT Technical Research Centre of Finland Ltd., Espoo 02044, Finland
[c] Department of Microbial Biotechnology, Helmholtz-Centre for Environmental Research-UFZ, Leipzig, Germany

ARTICLE INFO

Keywords:
Biocompatible
CO_2 reduction
Electrocatalysis
Indium
Single chamber

ABSTRACT

The electrochemical CO_2 reduction reaction (eCO_2RR) facilitates high rates and yields for the selective production of formate, a quintessential C1-compound that can serve as a valuable carbon and energy source for biosynthesis. The use of double-chamber (DC) electrochemical cells with membranes is deemed essential to avoid mixing of electrochemical products (i.e. anodic oxygen and cathodic formate) and thus cross-reactions that lower yields, Faradaic efficiency (FE) and effective rate. However, single-chamber (SC) setups for eCO_2RR can be more suitable to combine with bioprocesses. This work comprehensively evaluates, using different experimental setups, the conditions under which SC operation can obtain results comparable to DC systems. At a 50 mL scale, under biocompatible conditions, formate production in the SC setup achieved a 14 % reduction in the production rate (146 mg L^{-1} h^{-1} for SC and 170 mg L^{-1} h^{-1} for DC) and a 15 % decrease in FE (72.2 % in SC and 84.7 % in DC). The highest formate concentration produced in 24 h SC experiments was 1.8 g·L^{-1} with FE of 41 %, a concentration appropriate for fermentation processes. The SC operation of eCO_2RR to formate without a membrane could reduce energy losses and capital costs, although at the cost of an expected reduction in rate and FE.

1. Introduction

The electrochemical CO_2 reduction reaction (eCO_2RR) offers a highly appealing avenue for transforming this greenhouse gas into valuable feedstock for materials and fuels. Thus, eCO_2RR aims to close the human-induced carbon cycle and set ground for a circular bio-based economy. The eCO_2RR can be operated under ambient conditions at high rates and yields. This sets it apart from other CO_2 utilization technologies, such as biochemical, thermocatalytic, photosynthetic and photocatalytic processes [1–3].

Recent reviews highlight eCO_2RR for the cost-effective production of formate/formic acid and carbon monoxide [4–7], favouring electrochemical methods in terms of sustainability and efficiency [5,8]. Specifically, numerous researchers have demonstrated that high selectivity towards formate can be achieved with eCO_2RR employing certain metal cathodes [9–11]. Formate/formic acid plays a crucial role as a chemical building block in the pharmaceutical industry [12], acts as feedstock for preserving animal fodder [13], and as a fuel for fuel cells [14]. Furthermore, it also serves as a temporary storage molecule for electrolytic H_2 [15].

* Corresponding author.
E-mail address: JuanAntonio.Baeza@uab.cat (J.A. Baeza).
[1] Orcid: 0000-0002-2007-2277
[2] Orcid: 0000-0003-4812-3360
[3] Orcid: 0009-0004-6798-0979
[4] Orcid: 0000-0002-9427-8171
[5] Orcid: 0000-0003-1290-1669
[6] Orcid: 0000-0002-0014-4640
[7] Orcid: 0000-0002-3012-7964

https://doi.org/10.1016/j.jcou.2025.103136
Received 20 December 2024; Received in revised form 26 April 2025; Accepted 23 May 2025
Available online 30 May 2025

For the eCO_2RR in an aqueous electrolyte solution, indium (In) exhibits the highest selectivity to formate/formic acid production compared to tin (Sn), mercury (Hg), and lead (Pb) [16,17]. At In electrodes, eCO_2RR is highly efficient and achieves Faradaic efficiency (FE) exceeding 90 % [18]. This outstanding performance can be due to the high overpotential reported for undesired side reactions, such as the hydrogen evolution reaction (HER) [11,19]. However, Hegner *et al.* estimated the overpotentials for formate production (1.725 V) and HER (1.703 V) to be similar under biocompatible conditions [20], suggesting that the selectivity for eCO_2RR at In is caused by mechanical or kinetic processes rather than thermodynamics. Detweiler *et al.* further suggested that the increased FE at negative potential is due to In-oxide layer formation via anodization, suppressing HER by creating an In-OH layer on the electrode surface [21].

The eCO_2RR can be conducted in electrochemical cells using either a double-chamber (DC) setup with a membrane or a single-chamber (SC) setup without one. Membranes are typically considered necessary for separating the anolyte and catholyte. For eCO_2RR specifically, the use of DC shall prevent undesired crossover reactions such as anodic formate oxidation and cathodic oxygen reduction. This ought to increase the FE and allow different conditions for anolyte and catholyte (i.e., different pH). Prior studies have shown a high FE for formate production when utilizing in DC setups for eCO_2RR with ion exchange membranes. Ikeda *et al.* achieved 87.6 % of FE for formate production using an In catalyst with a cation exchange membrane [22], while Hori *et al.* achieved a slightly higher FE of 94.9 % using the same type of catalyst and membrane [19]. On the other hand, the use of membranes raises the resistance, which results in energy losses, leading to the need for higher cell voltages [23]. Thus, adding membranes also increases capital expenditure (CAPEX), the need for specialized equipment, and the added complexity of the system (such as intricate design, operational considerations, and maintenance) [24]. The alternative is using a membrane-free SC system to decrease the costs, although this could result in crossover reactions. Despite this trade-off, the simplicity of SC configurations makes them particularly attractive for integrated setups, where compatibility with downstream biological processes is crucial. While other architectures, such as membrane electrode assemblies, flow cells, and gas diffusion electrode (GDE) systems, are optimized for stand alone electrochemical performance and scalability, they often require more complex designs. In contrast, SC systems provide a more practical platform for direct coupling with microbial processes [25]. To our knowledge, no study has compared SC and DC setups for eCO_2RR under identical conditions.

For product extraction, the high solubility of formate in aqueous solutions demands an energy-intensive and consequently costly extraction process. This restriction can be addressed by merging the eCO_2RR with microbial synthesis. Once formate is produced with eCO_2RR, it can be utilized as a substrate for further conversion by formatotrophic microorganisms, producing value-added products [12,26]. This concept was first proposed by Li *et al.*, who described a process involving the eCO_2RR to formate, which was then converted into higher alcohols with an engineered strain of *Ralstonia eutropha* [26]. Given the well-established knowledge regarding the microbial conversion of C_1-compounds, this approach provides access to a wide range of potential products [12,27].

Coupling eCO_2RR and microbial catalysis in a single system is an unsolved problem that is far from simple. Performing abiotic eCO_2RR under biocompatible conditions needs systematic engineering to meet certain requirements, including sterility, pH, salinity, and tolerance to microbial media components, ensuring consistent integration with microbial processes. These compatibility factors are critical, as they affect both microbial growth and the electrochemical processes involved. For instance, microbial media components like yeast extract, trace elements, and phosphate can interfere with CO_2 reduction, significantly decreasing catalytic efficiency. Gimkiewicz et al. demonstrated that the presence of all three components reduced eCO_2RR performance at −1.6 V vs Ag/AgCl in carbonate buffer to just 11 % or less of the initial value (FE of 62 %) [28]. Additionally, maintaining sterility presents a challenge, as sterilization methods, whether steam, chemical or even γ-radiation, can alter the catalyst's layer, affecting its properties and compromising its efficiency, which ultimately reduces eCO_2RR efficiency [29].

Maintaining a pH that supports both microbial viability and electrochemical efficiency is also a key challenge in integrating eCO_2RR with microbial catalysis. For optimal microbial activity, a neutral or near-neutral pH is usually ideal [30]. However, pH also influences the competition between the eCO_2RR and the HER. In more acidic conditions, HER is favoured, which significantly reduces the FE of eCO_2RR. To avoid this, near-neutral or slightly alkaline conditions are typically preferred, as they inhibit HER and allow for more efficient CO_2 reduction [31]. Therefore, the reliance on proton concentration offers a way to adjust the selectivity of eCO_2RR according to pH levels. Research conducted in liquid electrolyte has pinpointed an optimal pH range for eCO_2RR, specifically from 7 to 10 [4]. A highly selective and efficient eCO_2RR to formate at pH 6.5 using DC has already been demonstrated by Hegner *et al.* [20], who explored the eCO_2RR for 1 h on In in DC, yielding an impressive FE of 94.5 % and a $r_{formate}$ of 0.061 mmol h^{-1} cm^{-2}. In a more recent development, Izadi et al. [32] reported a consistent FE of 82.3 % over the first few hours at pH 6.5 in a DC setup. However, since the optimal pH varies among microorganisms, further investigation across a broader pH range is necessary.

This work evaluates eCO_2RR to produce formate in SC configuration compared to conventional DC operation. The formate production that could be obtained in SC configuration is tested under biocompatible conditions, spanning different scales and interlaboratory experiments. Different applied potential and sterilizing procedures are tested with a view to its compatibility with subsequent microbial synthesis and to find the best conditions and the limitations that can be found when operating a SC configuration.

2. Material and methods

2.1. Experimental setup

To confirm the reproducibility of the experiments, setups from two different research groups were used. The first experimental setup (UFZ_configuration) was previously elucidated in detail by Gimkiewicz *et al.* and Hegner *et al.* [28,29,33]. In this study, experiments were conducted at two scales: 50 mL electrochemical cells as SC and DC and 1 L electrochemical reactors as DC. With the second setup (UAB_configuration), experiments were also conducted at two scales of 250 mL SC and 1 L SC.

The UFZ_configuration was used as a blueprint for setting up the UAB_configuration, which is described in detail as follows. Electrochemical pretreatment and In electrodeposition on the graphite backbone were conducted in a 300 mL vessel with a lid that included slots for each electrode and a port for sample and gassing (Fig. S1). All experiments using UAB_configuration were conducted under potentiostatic control with two potentiostats: NEV3-v2 (Nanoelectra, Spain) and VMP3 (BioLogic Science Instruments, France). The three-electrode setup consisted of a working electrode (WE), an Ag/AgCl reference electrode (RE, SE 11, 0.197 V vs standard hydrogen electrode (SHE) from Xylem Analytics Germany Sales Gmbh & Co. KG Sensortechnik Meinsberg, Germany), and a counter electrode (platinum sheet 2.5 cm × 2.5 cm, Merck, Spain).

The graphite rod used as the WE had 99 % purity (Ø 1.27 cm [actual geometric working surface area for 250 mL was 31 cm^2 and 41 cm^2 for 1 L], Fisher Scientific, Spain). Following mechanical and electrochemical pretreatment, In was electrodeposited on the graphite rods, as described previously [28]. For In electrodeposition, the graphite rod was linked to a rotating electrode holder (RW 20 D S000, IKA RW20 digital, Spain) via a custom-made adapter crafted from polylactic acid using a

3D printer. Throughout the measurements, CO_2 was constantly sparged at a rate of 100 mL min^{-1}. The electrolyte solution was continuously mixed using a magnetic stir bar rotating at 800 rpm. Experiments were conducted at 30°C utilizing a water bath.

2.2. Electrochemical CO_2 reduction to formate

For the electrochemical reduction of CO_2 to formate, a stirred vessel was filled with 250 mL or 980 mL of de-aerated $NaHCO_3$ (0.05 M, pH 6.5) and continuously sparged with CO_2. Chronoamperometry was performed to produce formate by applying a working electrode potential (E_{WE}) of −2.2 V vs Ag/AgCl unless otherwise stated. Samples of 1 mL were collected at 0, 1, 2, and 4 h for all formate production experiments. In the case of 24 h experiments, samples were taken at 0, 1, 2, 4, 20, 22, 24 h. These samples were then analysed using HPLC Dionex Ultimate3000 (Dionex-Thermo Fisher Scientific), which was equipped with a UV detector at 210 nm and an RI detector (Dionex-Thermo Fisher Scientific). The components were separated with an ionic exchange column ICSep ICE-COREGEL 87H3 (Transgenomic, Omaha, NE, USA). The mobile phase used was 6 mM sulphuric acid, and the separation was performed at a flow rate of 0.6 mL min^{-1}. The samples were promptly evaluated following sampling, and formate was the sole analyte detected in the liquid phase.

2.3. Sterilization and pH neutral conditions

To maintain a sterile environment in the 1 L setup as required for bioprocesses, steam or chemical sterilization methods were applied following the In electrodeposition on the graphite rods. For the steam sterilization, the In coated graphite backbone was assembled onto the WE inlet ports of the reactor lid, the gas sparger and the counter electrode was also assembled to the reactor vessel. Subsequently, the assembled reactor was placed inside the autoclave for steam sterilization at 121 °C for 20 min. Following the cooling, the reactor was equipped with a RE that underwent sterilization with 70 % ethanol for 10 min in a laminar flow box.

For the second method, chemical sterilization, the media and all the other reactor components underwent the same autoclaving procedure as before, while all the electrodes were submerged in a solution of 70 % ethanol for a duration of 10 min.

To analyse the effect of pH on eCO_2RR, the system performance using electrolyte solutions with different initial pH (4.5, 5, 5.5, 6, and 6.5) was studied. The solutions were prepared by adding the required amount of hydrochloric acid (HCl) to 0.05 M sodium bicarbonate ($NaHCO_3$).

2.4. Calculations

The FE of eCO_2RR to formate was determined (Eq. 1) with the charge transferred to formate (Q, Eq. 2), calculated from the actual mass (m) of formate produced, measured in grams, within the volume of the electrolyte solution (as determined by HPLC analysis) in relation to the total charge (Q_{total}) until the sampling point.

$$FE = \frac{Q}{Q_{total}} \cdot 100\% \quad (1)$$

$$Q = \frac{m}{M} \cdot z \cdot F \quad (2)$$

M represents the molar mass of formate (45 g mol^{-1}). The variable z is the number of electrons needed for eCO_2RR to formate (z = 2). F is the Faraday constant (96485 C mol^{-1}). Q_{total} (Eq. 3) can be determined by integrating the current (i) until the sampling point.

$$Q_{total}(t) = \int_0^t i(t)\, dt \quad (3)$$

The formate production rate ($r_{formate}$, Eq. 4, in mol cm^{-2} h^{-1}) was calculated with Δm as the increment of formate mass produced and normalized to the geometric surface area of the WE (A_{WEgeom} in cm^2).

$$r = \frac{\Delta m}{M \cdot A_{WE_{geom}} \cdot \Delta t} \quad (4)$$

Each experiment was conducted with a minimum of 3 independent replicates (n = 3) or more, as indicated in the text and captions. Independent replicates in this context mean that each individual replicate underwent the electrochemical cleaning, In electrodeposition and subsequent formate production.

3. Results and discussion

3.1. Using double vs. single chamber electrochemical cells for eCO_2RR

Fig. 1 compares the performance of eCO_2RR in SC and DC at 50 mL under the same operational conditions, using 0.05 mol L^{-1} $NaHCO_3$ (pH 6.5) as electrolyte and E_{WE} of −2.2 V vs Ag/AgCl. The performance metrics (FE and the amount of formate produced) decreased for SC vs DC. The FE achieved using the DC setup was 84.7 ± 1.8 %, while the SC exhibited 72.2 ± 6.0 % (14 % lower). Similarly, the amount of formate produced after 1 h was 170 ± 15.1 mg L^{-1} for DC and 146 ± 5.0 mg L^{-1} for SC (15 % lower). No significant changes in pH and conductivity were observed during the 1 h experiment (Table S1). It is worth mentioning that DC results closely coincide with the findings reported in other studies. Another evident outcome is the overall important level of reproducibility, as indicated by the minimal statistical variance. Thus, there was about 15 % decline in performance for eCO_2RR with the SC. A potential explanation for this SC system's performance, despite the risk of crossover reactions, may be attributed to the continuous sparging of CO_2. This constant flushing may ensure that most of the oxygen produced at the anode is expelled from the setup instead of being reduced at the cathode. In SC systems, the absence of a membrane allows ions from both electrochemical half cells to freely mix, which can lead to local pH shifts [34], and unstable ion transport [35]. These fluctuations may influence the reaction environment, especially on the local scale of the electrode, and reduce consistency. However, compared to DC systems, where such fluctuations are more controlled, their effect in SC appears to be minimal.

Compared to previous studies (Table 1), our study showed that the $r_{formate}$ in the DC configuration using In as catalyst reached 0.074 ± 0.008 mmol cm^{-2} h^{-1}, demonstrating an enhanced performance. Nevertheless, the $r_{formate}$ attained with the SC configuration (0.061 ± 0.003 mmol cm^{-2} h^{-1}) was 18 % lower than that with the DC configuration. This underscores that the SC setup can achieve comparable performance to the DC configuration. The current density is only

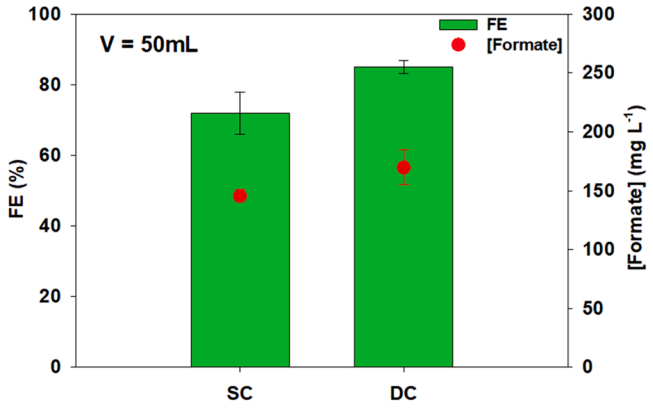

Fig. 1. eCO_2RR to formate in single chamber (SC) and double chamber (DC) at 50 mL scale (1 h). Reported values are means and the error bars represent the standard error of the mean (n = 3).

Table 1
Compilation of current density (j), FE and formate production rate ($r_{formate}$) obtained for double chamber (DC) and single chamber (SC) configurations. Reported values are mean values (n = 3) with standard error.

Config.	Catalyst	j (mA cm^{-2})	FE (%)	$r_{formate}$ (mmol cm^{-2} h^{-1})	E_{WE} (V vs Ag/AgCl)	Ref
DC	In	−27.8	72.5	0.0719	−1.9	[36]
DC	In	-	96.5	-	−0.9	[18]
DC	In	-	87.6	-	−2.0	[22]
DC	In	−5	94.9	-	−1.8	[19]
DC	In	−3.8	94.5	0.061	−2.2	[20]
DC	In	−1.14 ± 0.1	64.6 ± 6.8	0.013 ± 0.002	−1.6	[28]
DC	In	−4.68 ± 0.7	84.7 ± 1.8	0.074 ± 0.008	−2.2	This study
SC	In	−4.40 ± 1.1	72.2 ± 6.0	0.061 ± 0.003	−2.2	This study

reduced by about 6 % in SC vs DC, while the highest difference occurs in FE (15 % lower in SC vs DC). In any case, the $r_{formate}$ for the SC setup is similar to previous studies conducted in DC setup under the same E_{WE}. Specifically, the current density reported by Hegner et al. [20] (-3.8 mA cm^{-2}) in the DC setup was lower than that in this study, but resulted in $r_{formate}$ similar to this work in the SC setup.

Given the fundamental implications, this study reveals that crossover reactions had minimal influence on the eCO_2RR to formate. Oxygen reduction at the cathode could be a potential problem in a SC compared to a DC, but Hegner et al. [20] reported a higher selectivity of In for eCO_2RR to formate vs oxygen reduction reaction (ORR), ruling out a significant effect. Surprisingly, the influence of formate oxidation on FE appears to be minor under the conditions examined. Despite the higher standard oxidation potential of water (1.23 V) [37] compared to that of formate (0.22 V) [38], the oxidation of formate was minor due to the comparable but low concentrations produced with both SC and DC. This could be attributed to the limited availability of formate on the anode surface.

3.2. *Performance of eCO_2RR in single chamber electrochemical cells at different scales*

Fig. 2 shows a comparison of process performance of SC at three different scales (50 mL, 250 mL and 1 L) over the course of 1 h. A decrease in performance is noticeable in both 250 mL and 1 L reactors, with lower current density and formate production rates when compared to the 50 mL electrochemical cell. The $r_{formate}$ for the 250 mL and 1 L reactors is 26 % and 30 % lower, respectively, compared to the $r_{formate}$ of the 50 mL electrochemical cell. Despite this, FE remained consistently high across all scales throughout the 1 h period. Apart from

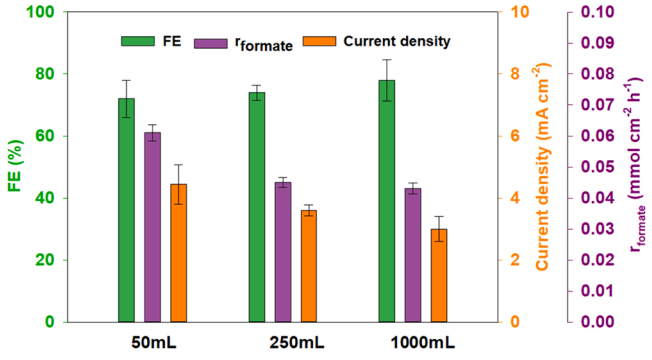

Fig. 2. Comparison of the performance of eCO_2RR to formate in SC at E_{WE}= -2.2 V vs Ag/AgCl for 1 h using three different scales: 50 mL, 250 mL and 1 L in 0.05 M $NaHCO_3$ electrolyte. Reported values are means, and the error bars represent the standard error of the mean.

the limitation of using identical electrode sizes for both scales, the increased distance between electrodes at the larger scale also contributed to lower current density. This greater separation causes variations in current density, even at the same applied potential.

One possible explanation for the variation in process performance could be the quality of the graphite rod backbone used. For the 50 mL electrochemical cell, high-quality graphite (> 99.997 % purity) was used, whereas, for practicality and lower CAPEX, graphite rods (99 % purity) were used for the 250 mL and 1 L setups. The presence of impurities in slightly lower grade graphite can have two different effects: non-conductive impurities may affect the electroactive surface area, while conductive impurities could act as alternative catalysts [39]. Moreover, these impurities may modify the features of the electrode, such as electrical resistance, which can lead to a decrease in $r_{formate}$ by affecting the current density.

Fig. 3 illustrates efficient formate production via eCO_2RR in SC at 250 mL and 1 L scale for 24 h. Again, the FE obtained during the initial 1 h period was relatively consistent across both scales. However, over time, the FE exhibited a gradual decrease. The decrease in FE for the 250 mL reactor was approximately 45 % after 24 h, while for the 1 L reactor, it was 32 %. Interestingly, a strong inverse linear correlation (R^2 up to 0.991) was observed between FE and formate concentration (Fig. 4). This indicates that as the concentration of formate increases, its oxidation at the counter electrode likely becomes more significant, thereby reducing both the formate retained in the medium and the overall FE. These results indicate that the extent of formate oxidation increases with higher formate concentrations. This gradual FE decrease raises concerns about the long-term sustainability of eCO_2RR. A lower FE necessitates more resource input, particularly electricity, to obtain the same amount of product. When also the carbon capture efficiency is affected, more CO_2 is required and, further, diluted product streams need additional downstream separation and recycling processes However, this issue can be mitigated by reducing the operation time to prevent a higher concentration in the medium. Furthermore, when aiming to integrate eCO_2RR with microbial synthesis, it is advantageous to maintain lower formate concentrations as higher levels can be toxic to many microorganisms [40]. It is also worth mentioning that this decrease in FE comes with the trade-off of working in a SC setup, which may provide compensatory benefits in scenarios where membrane addition is not feasible. Following a 24 h experimental period, a slight decrease in pH was observed, which can be attributed to the continuous flushing of CO_2. In contrast, conductivity exhibited a gradual rise over time, likely due to the generation of formate (Table S2).

A factor that may also contribute to the decrease in FE over time, beyond the effect of crossover reactions inherent to working in a SC setup, is its association with the HER. The HER competes with eCO_2RR, thereby reducing formate production efficiency [21,41]. HER may also contribute to In degradation by spalling off the metal catalyst [42]. However, the measurement of hydrogen in the headspace was not feasible during the experiment due to continuous CO_2 flushing but will be performed in the future. While our study was limited to 24 h operation, previous work demonstrated that In electrodes can sustain formate production for up to 72 h [32]. Although fluctuations in performance were observed after 24 h, likely due to competing HER, pH drift, and increased In leaching, formate production continued, indicating that the catalyst remained active under these conditions.

After 24 h, the formate concentration reached 1834 ± 87 mg L^{-1} in the 250 mL setup and 1327 ± 130 mg L^{-1} in the 1 L reactor. Notably, in this study, differences in scale resulted in variations not only in the reactor design but also in the surface area to volume ratios at different scales (Table S3). More precisely, the volume to surface area ratio at 250 mL was 3 times greater than at the 1 L scale, resulting in the increased formate concentration.

To ensure result reliability and verify outcomes independently, the performance of the 1 L SC eCO_2RR was also assessed by both research groups independently (Fig. S2). Despite differences in reactor

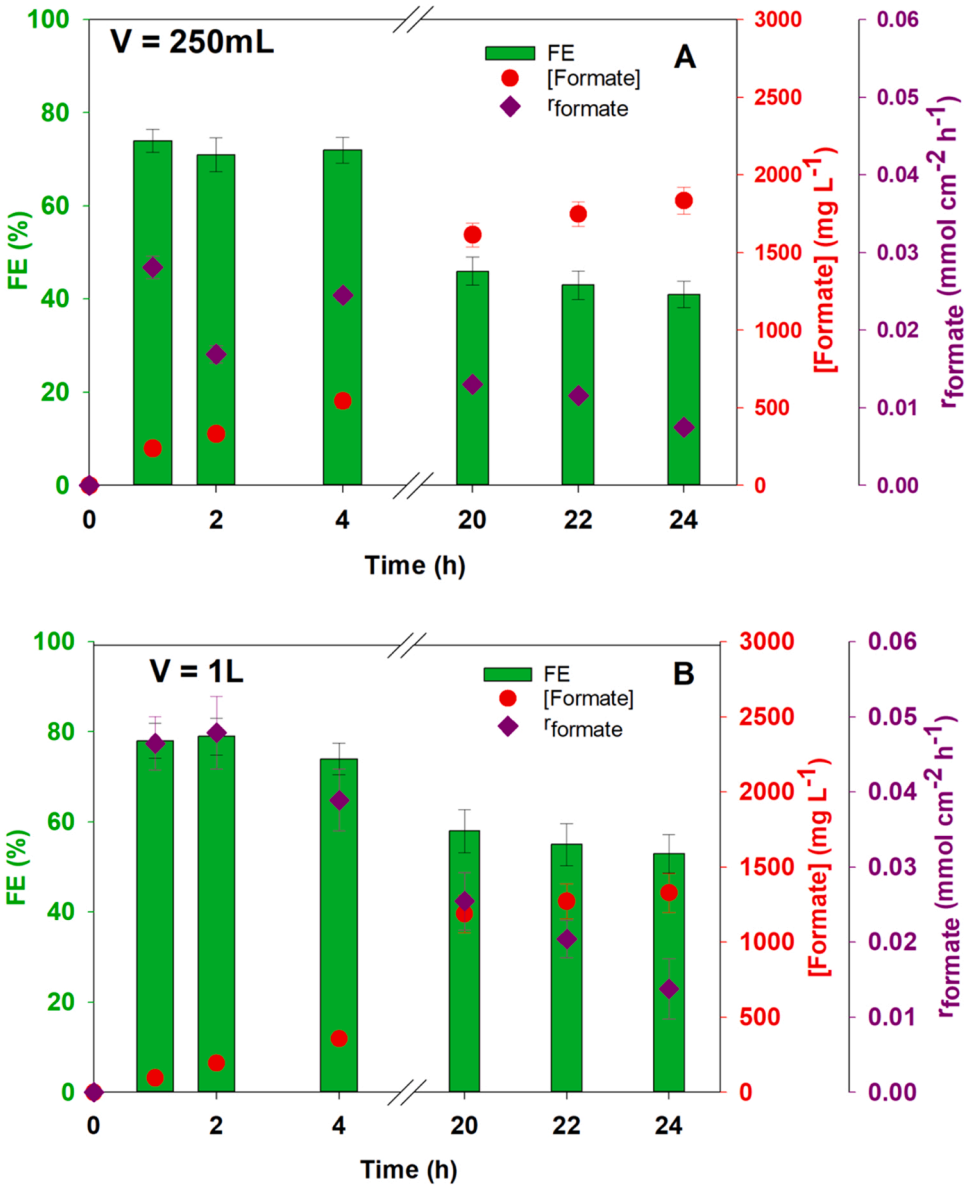

Fig. 3. eCO_2RR to formate at (A) 250 mL scale and (B) 1 L scale. Reported values are means and error bars represent the standard error of the mean (n = 3).

configurations, the performance remains remarkably similar. The FE achieved within 1 h using the UFZ_configuration was 73 ± 6.2 %, closely matching the value (74 ± 2.4 %) observed in the UAB_configuration. A decrease in FE was observed over time in experiments conducted with both configurations. After 24 h, the UFZ_configuration showed a 38 % reduction in FE, whereas the UAB_configuration demonstrated a 32 % reduction. This interlaboratory experiment, despite using different equipment, clearly demonstrated the reliability and accuracy of the SC setup. These consistent results suggest that the findings are generalizable across different configurations and conditions, enhancing their robustness and indicating broader applicability. Performing ring-tests, as already performed for the ORR [43], may be of interest for future studies.

3.3. *eCO_2RR to formate at different electrode potentials*

The efficiency of eCO_2RR is intricately linked to the E_{WE}, as shown for different materials such as Cu, Sn, and In [20,21,44–48]. Although a significant number of studies focused on the influence of E_{WE} on the FE and $r_{formate}$ in DC [20,32], no studies have been reported on E_{WE}'s influence on SC eCO_2RR. Therefore, the effect of E_{WE} on eCO_2RR using In electrodes was systematically examined in a 250 mL SC setup with 0.05 mol L^{-1} $NaHCO_3$ (pH 6.5) as electrolyte. As shown in Fig. 5, the correlation between the increase in current density and $r_{formate}$ underscores the essential role of E_{WE} as a critical parameter for driving the eCO_2RR to formate. Furthermore, it indicates that a more negative E_{WE} enhances $r_{formate}$, but the selectivity and therefore FE of the reaction toward formate is slightly lower for more negative potentials (-2.2 V).

The small relative decline for SC in FE (from 99 ± 0.7 % at −1.6 V to 74 ± 4.2 % at −2.2 V) may be attributed to the increased significance of formate oxidation at the anode and increased competition with HER at the cathode with a more negative E_{WE}. At more negative potentials HER may compete more effectively with eCO_2RR reducing overall selectivity as shown for mildly acid conditions, whereas at pH-neutral conditions this was not the case [20]. The same range of applied voltages (-1.6 V to −2.2 V) was also evaluated for DC configuration (50 mL) for 1 h (Table S4), to compare with SC setup (250 mL). In the DC setup, the $r_{formate}$ exhibited an increase with more negative potential, aligning with observations in the SC setup. However, the trend for the FE showed a slight rise with more negative E_{WE} in the DC setup, in complete contrast

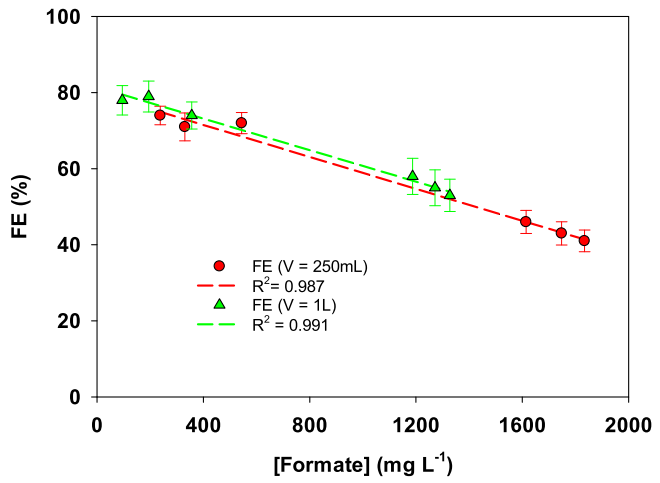

Fig. 4. Impact of formate concentration on FE at different scales. All experiments were conducted in 0.05 mol L^{-1} $NaHCO_3$ (pH 6.5) as electrolyte solution; n = 3; E_{WE} = -2.2 V. Reported values are means and the error bars represent the standard error of the mean.

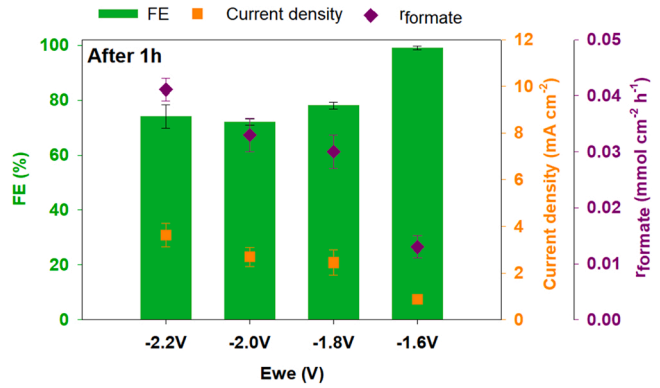

Fig. 5. Potential dependence of the SC eCO_2RR to formate at In electrodes (V=250 mL). Reported values are means (n = 3) and the error bars represent the standard error of the mean.

to what was observed for the SC setup. Likewise, Hegner *et al.* [29] examined comparable potentials using DC configuration and noticed a rise in $r_{formate}$ and current density and detected a shift in the selectivity of the reaction towards formate with a more negative E_{WE} with a FE of 93 % and $r_{formate}$ of 0.061 mmol cm^{-2} h^{-1} at −2.2 V.

Contrary to the results from the SC setup, there have been more reports of an increase in FE with decreasing E_{WE}, particularly in the context of anodized In electrodes. The anodization pretreatment of In electrodes, where an oxide layer is formed anodically on the electrode prior to CO_2 electrolysis, leads to the formation of an In-oxide layer [21]. Detweiler et al.[21] propose that an In-OH layer, resulting from an acid-base reaction at the electrode surface, impedes the HER at more negative potentials. Moreover, the FE for the formation of CO, a recognized intermediate or side product for In- and Sn-based electrodes, decreased at more negative cathode potentials. Agarwal *et al.* examined a range of E_{WE} between −1.5 V and −2.4 V (vs Ag/AgCl) employing Sn as a catalyst in DC for formate production [8]. They identified a narrow, optimized potential window between −1.8 V to −2.2 V (vs Ag/AgCl), beyond which the FE for formate production drops significantly to below 60 %.

The experiments in SC were extended for an additional 4 h of operation for each tested E_{WE} to evaluate its performance (Fig. S3). While the current density continued to increase with time, there was a slight decrease in FE, which was also observed in the case of $r_{formate}$ after 4 h. The decrease in $r_{formate}$ was particularly noticeable at −2.2 V, showing a decrease of 43 % after 4 h. Izadi et al. [32] examined the same potentials (-1.6 V to −2.2 V) to evaluate DC setup for eCO_2RR to formate production using a 50 mL setup (72 h). Contrary to the results obtained in this study (4 h), they observed a decrease in performance concerning FE and $r_{formate}$ at less negative potentials. For both SC and DC, the $r_{formate}$ shows similar trends across all potentials tested. In their study, using DC configuration, they reported $r_{formate}$ values of 0.01 mmol cm^{-2} h^{-1} at −1.6 V and 0.06 mmol cm^{-2} h^{-1} at −2.2 V after 4 h. In the present work, similar values of 0.015 mmol cm^{-2} h^{-1} ± 0.001 and 0.024 ± 0.001 mmol cm^{-2} h^{-1} at −1.6 V and −2.2 V were observed after 4 h, respectively.

3.4. *eCO₂RR for sterile operation and pH-neutral conditions*

When integrating eCO_2RR with biosynthesis, two different aspects should be considered: the need for sterility and the operation of eCO_2RR at biocompatible pH. Fig. 6 A illustrates that the production of formate was reduced when two sterilization methods were used (steam and chemical), in comparison to the unsterilized cathode. After 24 h, the production of formate for the non-sterilized reactor reached a concentration of 1.33 ± 0.28 g L^{-1}, surpassing the sterilization methods using steam (0.84 ± 0.21 g L^{-1}) and chemical (0.87 ± 0.13 g L^{-1}). Although there was a decrease in FE with time in all cases (Fig. 6 B), both steam and chemical sterilization resulted in reduced FE even after 1 h, with steam sterilization being 28 % lower and chemical sterilization being 22 % lower than unsterilized electrodes. This indicates that the sterilization methods affect the catalyst layer. While the performance difference between the two sterilization methods is not exceptionally high, the less complex method (chemical sterilization) appears to be the best option for the integration with microbial synthesis.

Steam sterilization, a commonly utilized method (ISO 13408) that requires exposure to high-temperature steam [49], has the potential to impact the In layer on the graphite rod. The comparison of photographic images captured prior and subsequent to the application of this procedure on the graphite rod indicates possible modifications in the chemical and physical characteristics of the In layer. The colour variation of the In layer was quite apparent, as observed visually (Fig. S4).

So far only Hegner *et al.* [29] assessed the performance of an In-layered graphite rod after steam sterilization for eCO_2RR using DC configuration. Their results are in accordance with our findings. They noted a nearly 23 % decrease in FE after 1 h with electrodes subjected to steam sterilization. In this study, the performance of eCO_2RR was also assessed using a DC with UFZ_configuration on a 1 L scale, employing steam sterilization for In electrodes. Comparable to the results obtained in SC, a reduction in FE due to steam sterilization was also noted in the DC configuration (Fig. S5). In the latter configuration, the decrease in FE was nearly 7 % with steam sterilized electrodes.

Regarding steam sterilisation, the SC approach offers an extra benefit. While steam effectively sterilizes In-layered graphite rods, sterilizing the membrane adds additional intricacy to the overall electrode sterilization procedure. Hegner et al. [33] utilized dry heat sterilization by enclosing the counter electrode chamber with a graphite rod in a glass vessel, effectively preventing any contact between water vapor and the ion exchange membrane. This method can be bypassed when working with a SC setup. For instance, in fermentation processes, chemical sterilization is commonly employed for pH and oxygen probes in bioreactors to avoid microbial contamination, ensuring probe integrity during fermentation [50]. However, the use of this sterilizing technique on In electrodes in this study, employing a 70 % ethanol solution for 10 min, resulted in adverse effects on the In-catalyst layer.

The impact of pH on the performance of eCO_2RR in terms of FE and formate production is depicted in Fig. 7. The increase in FE and the quantity of produced formate is apparent at a more neutral pH. The impact of the competing HER on eCO_2RR was quite significant at lower pH, resulting in a 58 % decrease in FE at pH 4.5 compared to pH 6.5 after

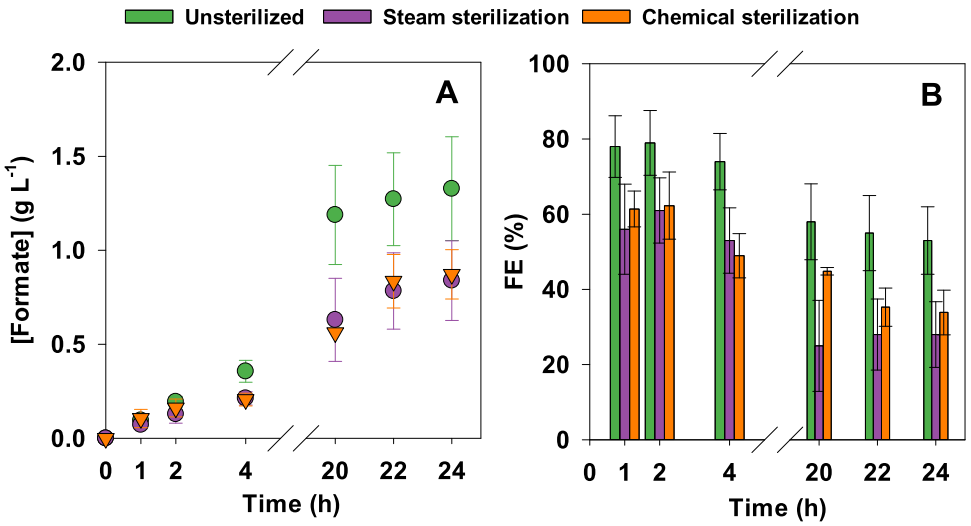

Fig. 6. (A) Formate production and (B) FE of eCO_2RR in the 1 L reactor in SC without and with steam and chemical sterilization (UAB_configuration). Reported values are means and error bars represent the standard error of the mean (n = 3).

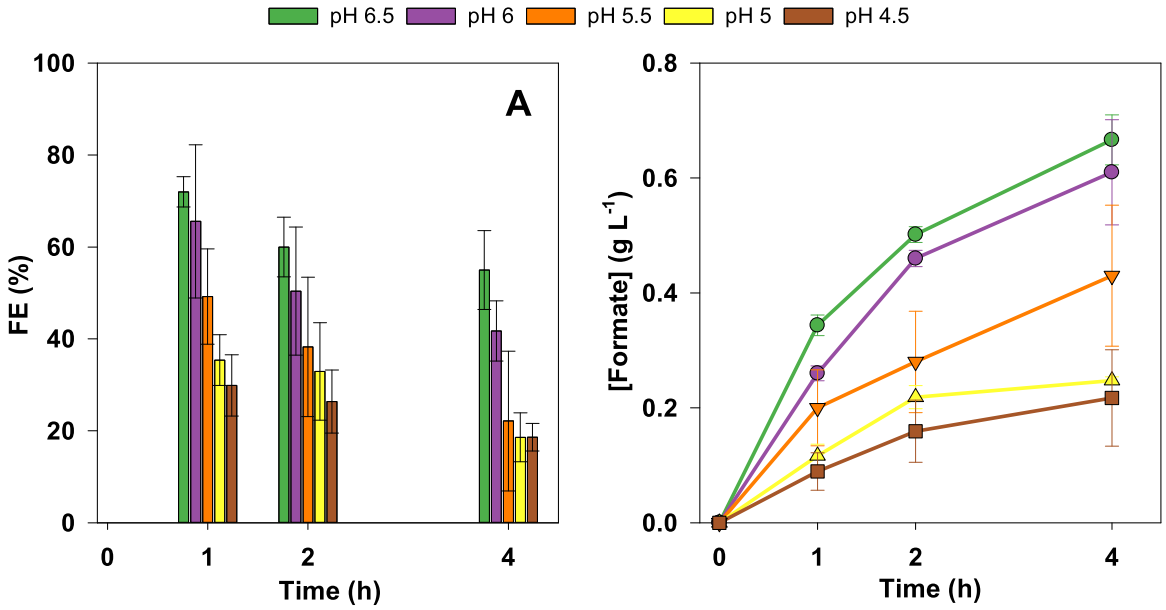

Fig. 7. (A) FE and (B) formate production of SC eCO_2RR under different pH conditions (250 mL). Reported values are means and error bars represent the standard error of the mean (n = 3).

1 h, and this decline persisted over time.

After 4 h, the final formate concentration at pH 6.5 reached 0.67 ± 0.05 g L^{-1}, which was 67 % higher than the concentration obtained at pH 4.5. These findings were anticipated, as they align with prior studies showing that increased acidity is known to enhance the HER significantly [51]. Nevertheless, the conductivity, as measured for various initial pH, exhibited a gradual increase over time, suggesting the formation of formate (Table S5). A slight decrease in pH was also observed over time (Table S6). Thus, pH levels lower than 4.5 were not tested as also previous studies have reported that even exceptionally effective eCO_2RR catalysts may fail under highly acidic conditions [52].

As mentioned earlier, the decline in performance over time may be attributed to the shift in local pH at the electrode surface. This shift can have an impact on the reaction pathways, selectivity, and stability [53]. Factors such as HER competition, In leaching, pH changes at the electrode surface may coexist and interact with each other, presenting a significant challenge in designing stable eCO_2RR electrolysers for long term use. Most studies were performed under neutral to alkaline conditions to mitigate HER competition [20,28,29,32,33,54–57]. However, in contrast to our study, only a few studies have obtained satisfactory results under acidic conditions. Recently, Huang *et al.* used Cu as a catalyst in a strong acid electrolyte solution achieving a current density of 1.2 A cm^{-2} and a FE of 50 % for multi-carbon products [58]. Whipple et al. [59] explored different pH conditions (4, 7, 10) for eCO_2RR to formate using a Sn catalyst on a GDE within a microfluidic electrochemical cell. They observed that lowering the pH enhanced current density and selectivity for formic acid due to reduced cathodic polarization losses, enabling higher current densities.

The pH of the electrolyte solution significantly impacts the eCO_2RR and the subsequent separation of formate/formic acid. The choice of separation process is contingent on the acid dissociation state. Although electrochemists commonly employ formic acid and formate interchangeably, their equilibrium directly affects the selection of a suitable downstream process. Ramdin et al. [31] reviewed the impact of pH on

the downstream separation processes and their economic aspects, suggesting liquid−liquid extraction for formic acid and electrodialysis for formate. However, both methods are complex and costly.

3.5. Future perspectives for the SC set-up

Attaining high FE at high current densities is a sought-after trait for any commercial eCO_2RR process. This study achieved, for the first time, high FE at a less negative potential (-1.6 V) in a SC setup at different scales and under various operational conditions. Operating at a less negative potential decreases the energy requirements at the expense of producing less formate (340 mg L^{-1} for −1.6 V) than at a more negative potential (650 mg L^{-1} for −2.2 V) after 4 h. Hence, a trade-off exists between achieving high FE and maximizing formate production for SC eCO_2RR. Nonetheless, to further improve the performance in terms of $r_{formate}$, the utilization of 3D electrodes is highly appealing [60]. For instance, bed electrodes, unlike the graphite rod employed in this study, can enhance current densities and overall reaction rates within the reactor volume. Additionally, the use of GDE instead of monolithic electrodes is highly appealing. GDEs offer a large electroactive surface area, enabling operation at higher current densities, while also enhancing the three-phase boundary area to mitigate mass transfer limitations and promote eCO_2RR. Nevertheless, the performance of eCO_2RR is still constrained by the long-term stability of the electrocatalyst (in this case, In on the graphite rod). Thus, it is essential to explore alternative electrode materials such as Sn or Cu, which are less critical [61] or other catalysts like $MoSi_2N_4$, which have shown promise for their stability and electrochemical performance in various catalytic processes [62]. Additionally, optimizing operational conditions to align more closely with industrial implementation should also be investigated [63].

Given the paramount importance of sterility and pH when linking eCO_2RR and microbial catalysis, the impact of these factors on SC eCO_2RR performance was also investigated. While both steam and chemical sterilization methods can ensure sterility, their implementation impact performance compared to the unsterilized system. This study shows that chemical sterilisation has a similar impact on formate production as steam sterilisation and is much more efficient from a practical point of view, especially when membranes are involved. Nevertheless, ensuring the sterility of the electrobioreactor is crucial, and thus alternatives could be evaluated. The γ radiation presents a potential alternative for sterilizing electrodes. Although cost-effective (excluding initial setup) and capable of deep penetration without leaving toxic residues, there is an evidence of detrimental effects on sterilized products, such as material degradation and chemical changes [64, 65]. However, the impact of γ radiation on electrodes for eCO_2RR remains unexplored.

4. Conclusions

This study demonstrates for the first time formate production via eCO_2RR using In as a catalyst in a single chamber setup across multiple scales (50 mL, 250 mL and 1 L). To assess the reliability of the SC setup, its performance was benchmarked against the DC configuration. Under the same conditions, the DC configuration yielded a $r_{formate}$ of 0.074 ± 0.008 mmol cm^{-2} h^{-1} with a FE of 84.7 ± 1.8 %. The SC configuration yielded 17 % lower $r_{formate}$ of 0.061 ± 0.003 mmol cm^{-2} h^{-1} with a FE of 72.2 ± 6.0 %, indicating that the use of membranes is not essential for formate production via eCO_2RR, but some reduction in rate and FE is to be expected. In the SC setup, applying more negative potentials (-2.2 V vs Ag/AgCl) resulted in higher current density and $r_{formate}$, albeit at the expense of slightly reduced selectivity. An independent inter-laboratory test by two research groups showed similar FEs (73 ± 6.2 % vs 74 ± 2.4 % at 1 h) and similar reductions of FE after 24 h (38 % and 32 % reduction) for the SC set-up.

Two sterilization methods (steam and chemical) were benchmarked against a non-sterilized setup. Both methods were found to have detrimental effects on the eCO_2RR performance, resulting in reduced FE. Steam sterilization led to 28 % reduction, while chemical sterilization resulted in a 22 % compared to unsterilized electrodes. The significance of pH in regulating the selectivity of eCO_2RR was also evident, with the more kinetically favourable HER outcompeting eCO_2RR and causing a 58 % decrease in FE at pH 4.5 compared to pH 6.5.

CRediT authorship contribution statement

Zainab Ul: Conceptualization, Methodology, Formal analysis, Investigation, Visualization, Data curation, Writing – original draft. **Mira Sulonen:** Conceptualization, Methodology Formal analysis, Supervision, Writing – review & editing. **Philip Haus:** Investigation, Formal analysis. **Paniz Izadi:** Conceptualization, Methodology, Formal analysis, Supervision, Writing – review & editing. **Juan Antonio Baeza:** Conceptualization, Methodology, Formal analysis, Supervision, Writing – review & editing. **Falk Harnisch:** Conceptualization, Methodology, Formal analysis, Supervision, Writing – review & editing. **Albert Guisasola:** Conceptualization, Methodology, Formal analysis, Supervision, Funding acquisition, Writing – review & editing.

Declaration of Competing Interest

The authors declare that they have no known competing financial interests or personal relationships that could have appeared to influence the work reported in this paper.

Acknowledgements

The authors acknowledge the support of the VIVALDI project that has received funding from the European Union's Horizon 2020 research and innovation programme under grant agreement 101000441. This work was supported by the Helmholtz-Association in the frame of the Integration Platform "Tapping nature's potential for sustainable production and a healthy environment" at the UFZ. The authors would like to thank Carles Contreras Rafanell for his technical assistance in some of the experimental work carried out at the UAB. The authors from UAB are members of the GENOCOV research group (Grup de Recerca Consolidat de la Generalitat de Catalunya, 2021 SGR 515, www.genocov.com). Albert Guisasola acknowledges the funding from the ICREA Academia grant.

Appendix A. Supporting information

Supplementary data associated with this article can be found in the online version at doi:10.1016/j.jcou.2025.103136.

Data availability

Data will be made available on request.

References

[1] C. Ren, W. Ni, H. Li, Recent progress in electrocatalytic reduction of CO2, Catalysts 13 (2023) 644, https://doi.org/10.3390/catal13040644.
[2] S. Yoshino, T. Takayama, Y. Yamaguchi, A. Iwase, A. Kudo, CO $_2$ reduction using water as an electron donor over heterogeneous photocatalysts aiming at artificial photosynthesis, Acc. Chem. Res. 55 (2022) 966–977, https://doi.org/10.1021/acs.accounts.1c00676.
[3] Z. Sun, J. Dong, C. Chen, S. Zhang, Y. Zhu, Photocatalytic and electrocatalytic CO $_2$ conversion: from fundamental principles to design of catalysts, J. Chem. Tech. Biotech. 96 (2021) 1161–1175, https://doi.org/10.1002/jctb.6653.
[4] Electrochemical CO_2 reduction – a critical view on fundamentals, materials and applications, Chimia 69 (2015) 769, https://doi.org/10.2533/chimia.2015.769.
[5] C. Oloman, H. Li, Electrochemical processing of carbon dioxide, ChemSusChem 1 (2008) 385–391, https://doi.org/10.1002/cssc.200800015.
[6] A.J. Martín, G.O. Larrazábal, J. Pérez-Ramírez, Towards sustainable fuels and chemicals through the electrochemical reduction of CO $_2$: lessons from water

electrolysis, Green Chem. 17 (2015) 5114–5130, https://doi.org/10.1039/C5GC01893E.
[7] S. Verma, B. Kim, H.-R. "Molly" Jhong, S. Ma, P.J.A. Kenis, A gross-margin model for defining technoeconomic benchmarks in the electroreduction of CO_2, ChemSusChem 9 (2016) 1972–1979, https://doi.org/10.1002/cssc.201600394.
[8] A.S. Agarwal, Y. Zhai, D. Hill, N. Sridhar, The electrochemical reduction of carbon dioxide to formate/formic acid: engineering and economic feasibility, ChemSusChem 4 (2011) 1301–1310, https://doi.org/10.1002/cssc.201100220.
[9] K.S. Udupa, G.S. Subramanian, H.V.K. Udupa, The electrolytic reduction of carbon dioxide to formic acid, Electrochim. Acta 16 (1971) 1593–1598, https://doi.org/10.1016/0013-4686(71)80028-2.
[10] H. Rabiee, L. Ge, X. Zhang, S. Hu, M. Li, Z. Yuan, Gas diffusion electrodes (GDEs) for electrochemical reduction of carbon dioxide, carbon monoxide, and dinitrogen to value-added products: a review, Energy Environ. Sci. 14 (2021) 1959–2008, https://doi.org/10.1039/D0EE03756G.
[11] M. Todoroki, K. Hara, A. Kudo, T. Sakata, Electrochemical reduction of high pressure CO2 at Pb, Hg and In electrodes in an aqueous KHCO3 solution, J. Electroanal. Chem. 394 (1995) 199–203, https://doi.org/10.1016/0022-0728(95)04010-L.
[12] A. Bar-Even, E. Noor, A. Flamholz, R. Milo, Design and analysis of metabolic pathways supporting formatotrophic growth for electricity-dependent cultivation of microbes, Biochim. Et. Biophys. Acta (BBA) Bioenerg. 1827 (2013) 1039–1047, https://doi.org/10.1016/j.bbabio.2012.10.013.
[13] S.C. Ricke, D.K. Dittoe, K.E. Richardson, Formic acid as an antimicrobial for poultry production: a review, Front. Vet. Sci. 7 (2020) 563, https://doi.org/10.3389/fvets.2020.00563.
[14] N.M. Aslam, M.S. Masdar, S.K. Kamarudin, W.R.W. Daud, Overview on direct formic acid fuel cells (DFAFCs) as an energy sources, APCBEE Procedia 3 (2012) 33–39, https://doi.org/10.1016/j.apcbee.2012.06.042.
[15] Y. Xiong, B. Wei, M. Wu, B. Hu, F. Zhu, J. Hao, W. Shi, Rapid synthesis of amorphous bimetallic copper-bismuth electrocatalysts for efficient electrochemical CO2 reduction to formate in a wide potential window, J. CO2 Util. 51 (2021) 101621, https://doi.org/10.1016/j.jcou.2021.101621.
[16] M. Jitaru, D.A. Lowy, M. Toma, B.C. Toma, L. Oniciu, Electrochemical reduction of carbon dioxide on flat metallic cathodes, J. Appl. Electochem. 27 (1997) 875–889, https://doi.org/10.1023/A:1018441316386.
[17] C.M. Sánchez-Sánchez, V. Montiel, D.A. Tryk, A. Aldaz, A. Fujishima, Electrochemical approaches to alleviation of the problem of carbon dioxide accumulation, Pure Appl. Chem. 73 (2001) 1917–1927, https://doi.org/10.1351/pac200173121917.
[18] B. Zha, C. Li, J. Li, Efficient electrochemical reduction of CO2 into formate and acetate in polyoxometalate catholyte with indium catalyst, J. Catal. 382 (2020) 69–76, https://doi.org/10.1016/j.jcat.2019.12.010.
[19] Y. Hori, H. Wakebe, T. Tsukamoto, O. Koga, Electrocatalytic process of CO selectivity in electrochemical reduction of CO2 at metal electrodes in aqueous media, Electrochim. Acta 39 (1994) 1833–1839, https://doi.org/10.1016/0013-4686(94)85172-7.
[20] R. Hegner, L.F.M. Rosa, F. Harnisch, Electrochemical CO2 reduction to formate at indium electrodes with high efficiency and selectivity in pH neutral electrolytes, Appl. Catal. B Environ. 238 (2018) 546–556, https://doi.org/10.1016/j.apcatb.2018.07.030.
[21] Z.M. Detweiler, J.L. White, S.L. Bernasek, A.B. Bocarsly, Anodized Indium metal electrodes for enhanced carbon dioxide reduction in aqueous electrolyte, Langmuir 30 (2014) 7593–7600, https://doi.org/10.1021/la501245p.
[22] S. Ikeda, T. Takagi, K. Ito, Selective formation of formic acid, oxalic acid, and carbon monoxide by electrochemical reduction of carbon Dioxide, Bull. Chem. Soc. Jpn. 60 (1987) 2517–2522, https://doi.org/10.1246/bcsj.60.2517.
[23] Y. Zhao, L. Duan, Research on measuring pure membrane electrical resistance under the effects of salinity gradients and diffusion boundary layer and double layer resistances, Membranes 12 (2022) 816, https://doi.org/10.3390/membranes12080816.
[24] C.H. Lo, E. McAdam, S. Judd, The cost of a small membrane bioreactor, Water Sci. Technol. 72 (2015) 1739–1746, https://doi.org/10.2166/wst.2015.394.
[25] D. Ewis, M. Arsalan, M. Khaled, D. Pant, M.M. Ba-Abbad, A. Amhamed, M.H. El-Naas, Electrochemical reduction of CO2 into formate/formic acid: A review of cell design and operation, Sep. Purif. Technol. 316 (2023) 123811, https://doi.org/10.1016/j.seppur.2023.123811.
[26] H. Li, P.H. Opgenorth, D.G. Wernick, S. Rogers, T.-Y. Wu, W. Higashide, P. Malati, Y.-X. Huo, K.M. Cho, J.C. Liao, Integrated electromicrobial conversion of CO_2 to higher alcohols, Science 335 (2012), https://doi.org/10.1126/science.1217643, 1596–1596.
[27] J. Schrader, M. Schilling, D. Holtmann, D. Sell, M.V. Filho, A. Marx, J.A. Vorholt, Methanol-based industrial biotechnology: current status and future perspectives of methylotrophic bacteria, Trends Biotechnol. 27 (2009) 107–115, https://doi.org/10.1016/j.tibtech.2008.10.009.
[28] C. Gimkiewicz, R. Hegner, M.F. Gutensohn, C. Koch, F. Harnisch, Study of electrochemical reduction of CO_2 for future use in secondary microbial electrochemical technologies, ChemSusChem 10 (2017) 958–967, https://doi.org/10.1002/cssc.201601675.
[29] R. Hegner, K. Neubert, L.F.M. Rosa, F. Harnisch, Engineering electrochemical CO_2 reduction to formate under bioprocess-compatible conditions to bioreactor scale, ChemElectroChem 6 (2019) 3731–3735, https://doi.org/10.1002/celc.201900526.
[30] Q. Jin, M.F. Kirk, pH as a primary control in environmental microbiology: 1. Thermodynamic perspective, Front. Environ. Sci. 6 (2018) 21, https://doi.org/10.3389/fenvs.2018.00021.
[31] M. Ramdin, A.R.T. Morrison, M. De Groen, R. Van Haperen, R. De Kler, L.J.P. Van Den Broeke, J.P.M. Trusler, W. De Jong, T.J.H. Vlugt, High pressure electrochemical reduction of CO_2 to formic acid/formate: a comparison between bipolar membranes and cation exchange membranes, Ind. Eng. Chem. Res. 58 (2019) 1834–1847, https://doi.org/10.1021/acs.iecr.8b04944.
[32] P. Izadi, A. Kas, P. Haus, F. Harnisch, On the stability of electrochemical CO2 reduction reaction to formate at indium electrodes at biocompatible conditions, Electrochim. Acta 462 (2023) 142733, https://doi.org/10.1016/j.electacta.2023.142733.
[33] R. Hegner, K. Neubert, C. Kroner, D. Holtmann, F. Harnisch, Coupled electrochemical and microbial catalysis for the production of polymer bricks, ChemSusChem 13 (2020) 5295–5300, https://doi.org/10.1002/cssc.202001272.
[34] M.H. Hicks, W. Nie, A.E. Boehme, H.A. Atwater, T. Agapie, J.C. Peters, Electrochemical CO_2 reduction in acidic electrolytes: spectroscopic evidence for local pH gradients, J. Am. Chem. Soc. 146 (2024) 25282–25289, https://doi.org/10.1021/jacs.4c09512.
[35] S. Chinnathambi, M. Ramdin, T.J.H. Vlugt, Mass transport limitations in electrochemical conversion of CO2 to formic acid at high pressure, Electrochem 3 (2022) 549–569, https://doi.org/10.3390/electrochem3030038.
[36] B. Bohlen, D. Wastl, J. Radomski, V. Sieber, L. Vieira, Electrochemical CO2 reduction to formate on indium catalysts prepared by electrodeposition in deep eutectic solvents, Electrochem. Commun. 110 (2020) 106597, https://doi.org/10.1016/j.elecom.2019.106597.
[37] R. Sen, S. Das, A. Nath, P. Maharana, P. Kar, F. Verpoort, P. Liang, S. Roy, Electrocatalytic water oxidation: an overview with an example of translation from lab to market, Front. Chem. 10 (2022) 861604, https://doi.org/10.3389/fchem.2022.861604.
[38] S.J. Folkman, J. González-Cobos, S. Giancola, I. Sánchez-Molina, J.R. Galán-Mascarós, Benchmarking catalysts for formic acid/formate electrooxidation, Molecules 26 (2021) 4756, https://doi.org/10.3390/molecules26164756.
[39] I.D. Kashcheev, K.G. Zemlyanoi, V.M. Ust'yantsev, S.A. Pomortsev, Study of the structure and properties of graphites for refractory production. Part 1. Physicochemical study of graphites from different deposits, Refract Ind. Ceram. 56 (2016) 577–582, https://doi.org/10.1007/s11148-016-9891-z.
[40] L. Zeng, Z. Si, X. Zhao, P. Feng, J. Huang, X. Long, Y. Yi, Metabolome analysis of the response and tolerance mechanisms of Saccharomyces cerevisiae to formic acid stress, Int. J. Biochem. Cell Biol. 148 (2022) 106236, https://doi.org/10.1016/j.biocel.2022.106236.
[41] Z. Xia, M. Freeman, D. Zhang, B. Yang, L. Lei, Z. Li, Y. Hou, Highly selective electrochemical conversion of CO_2 to HCOOH on dendritic indium foams, ChemElectroChem 5 (2018), https://doi.org/10.1002/celc.201701294.
[42] F. Bienen, A. Löwe, J. Hildebrand, S. Hertle, D. Schonvogel, D. Kopljar, N. Wagner, E. Klemm, K.A. Friedrich, Degradation study on tin- and bismuth-based gas-diffusion electrodes during electrochemical CO2 reduction in highly alkaline media, J. Energy Chem. 62 (2021) 367–376, https://doi.org/10.1016/j.jechem.2021.03.050.
[43] F. Jaouen, J. Herranz, M. Lefèvre, J.-P. Dodelet, U.I. Kramm, I. Herrmann, P. Bogdanoff, J. Maruyama, T. Nagaoka, A. Garsuch, J.R. Dahn, T. Olson, S. Pylypenko, P. Atanassov, E.A. Ustinov, Cross-laboratory experimental study of non-noble-metal electrocatalysts for the oxygen reduction reaction, ACS Appl. Mater. Interfaces 1 (2009) 1623–1639, https://doi.org/10.1021/am900219g.
[44] J. Durst, A. Siebel, C. Simon, F. Hasché, J. Herranz, H.A. Gasteiger, New insights into the electrochemical hydrogen oxidation and evolution reaction mechanism, Energy Environ. Sci. 7 (2014) 2255–2260, https://doi.org/10.1039/C4EE00440J.
[45] J.L. White, A.B. Bocarsly, Enhanced carbon dioxide reduction activity on indium-based nanoparticles, J. Electrochem. Soc. 163 (2016) H410–H416, https://doi.org/10.1149/2.0681606jes.
[46] Y. Hori, A. Murata, R. Takahashi, Formation of hydrocarbons in the electrochemical reduction of carbon dioxide at a copper electrode in aqueous solution, J. Chem. Soc., Faraday Trans. 85 (1989) 2309, https://doi.org/10.1039/f19898502309.
[47] S. Zhang, P. Kang, T.J. Meyer, Nanostructured tin catalysts for selective electrochemical reduction of carbon dioxide to formate, J. Am. Chem. Soc. 136 (2014) 1734–1737, https://doi.org/10.1021/ja4113885.
[48] W. Lv, J. Zhou, F. Kong, H. Fang, W. Wang, Porous tin-based film deposited on copper foil for electrochemical reduction of carbon dioxide to formate, Int. J. Hydrog. Energy 41 (2016) 1585–1591, https://doi.org/10.1016/j.ijhydene.2015.11.100.
[49] ISO 13408-1:2023(en), Aseptic Processing of Health Care Products — Part 1: General Requirements, (n.d.). ⟨https://www.iso.org/obp/ui#iso:std:iso:13408:-1:ed-3:v1:en⟩ (accessed June 30, 2024).
[50] C. Busse, P. Biechele, I. De Vries, K.F. Reardon, D. Solle, T. Scheper, Sensors for disposable bioreactors, Eng. Life Sci. 17 (2017) 940–952, https://doi.org/10.1002/elsc.201700049.
[51] Y. Ruiz, J.A. Baeza, A. Guisasola, Enhanced performance of bioelectrochemical hydrogen production using a pH control strategy, ChemSusChem 8 (2015) 389–397, https://doi.org/10.1002/cssc.201403083.
[52] C. Delacourt, P. Ridgway, J. Kerr, J. Newman, Design of an electrochemical cell making syngas ($CO + H_2$) from CO_2 and H_2O reduction at room temperature, 197–197, Meet. Abstr. MA2007-02 (2007), https://doi.org/10.1149/MA2007-02/3/197.
[53] A. Senocrate, C. Battaglia, Electrochemical CO2 reduction at room temperature: status and perspectives, J. Energy Storage 36 (2021) 102373, https://doi.org/10.1016/j.est.2021.102373.
[54] M.H. Do, H.H. Ngo, W.S. Guo, Y. Liu, S.W. Chang, D.D. Nguyen, L.D. Nghiem, B. J. Ni, Challenges in the application of microbial fuel cells to wastewater treatment

and energy production: a mini review, Sci. Total Environ. 639 (2018) 910–920, https://doi.org/10.1016/j.scitotenv.2018.05.136.
[55] A.S. Varela, The importance of pH in controlling the selectivity of the electrochemical CO2 reduction, Curr. Opin. Green Sustain. Chem. 26 (2020) 100371, https://doi.org/10.1016/j.cogsc.2020.100371.
[56] S.R. Narayanan, B. Haines, J. Soler, T.I. Valdez, Electrochemical conversion of carbon dioxide to formate in alkaline polymer electrolyte membrane cells, J. Electrochem. Soc. 158 (2011) A167, https://doi.org/10.1149/1.3526312.
[57] P. Bumroongsakulsawat, G.H. Kelsall, Effect of solution pH on CO: formate formation rates during electrochemical reduction of aqueous CO2 at Sn cathodes, Electrochim. Acta 141 (2014) 216–225, https://doi.org/10.1016/j.electacta.2014.07.057.
[58] J.E. Huang, F. Li, A. Ozden, A. Sedighian Rasouli, F.P. García De Arquer, S. Liu, S. Zhang, M. Luo, X. Wang, Y. Lum, Y. Xu, K. Bertens, R.K. Miao, C.-T. Dinh, D. Sinton, E.H. Sargent, CO_2 electrolysis to multicarbon products in strong acid, Science 372 (2021) 1074–1078, https://doi.org/10.1126/science.abg6582.
[59] D.T. Whipple, E.C. Finke, P.J.A. Kenis, Microfluidic reactor for the electrochemical reduction of carbon dioxide: the effect of pH, Electrochem. Solid-State Lett. 13 (2010) B109, https://doi.org/10.1149/1.3456590.
[60] S. (Rob) Hui, N. Shaigan, V. Neburchilov, L. Zhang, K. Malek, M. Eikerling, P. D. Luna, Three-dimensional cathodes for electrochemical reduction of CO2: from macro- to nano-engineering, Nanomaterials 10 (2020) 1884, https://doi.org/10.3390/nano10091884.
[61] Y. Pei, H. Zhong, F. Jin, A brief review of electrocatalytic reduction of CO_2—materials, reaction conditions, and devices, Energy Sci. Eng. 9 (2021) 1012–1032, https://doi.org/10.1002/ese3.935.
[62] W. Xun, X. Yang, Q.-S. Jiang, M.-J. Wang, Y.-Z. Wu, P. Li, Single-atom-anchored two-dimensional $MoSi_2N_4$ monolayers for efficient electroreduction of CO_2 to formic acid and methane, ACS Appl. Energy Mater. 6 (2023) 3236–3243, https://doi.org/10.1021/acsaem.2c03687.
[63] S. Garg, M. Li, A.Z. Weber, L. Ge, L. Li, V. Rudolph, G. Wang, T.E. Rufford, Advances and challenges in electrochemical CO_2 reduction processes: an engineering and design perspective looking beyond new catalyst materials, J. Mater. Chem. A 8 (2020) 1511–1544, https://doi.org/10.1039/C9TA13298H.
[64] C.R. Harrell, V. Djonov, C. Fellabaum, V. Volarevic, Risks of using sterilization by gamma radiation: the other side of the coin, Int. J. Med. Sci. 15 (2018) 274–279, https://doi.org/10.7150/ijms.22644.
[65] M.R. Saghee, T. Sandle, Application of sterilization by gamma radiation for single-use disposable technologies in the biopharmaceutical sector, Pharm. Technol. (2012).